STEADY LONGITUDINAL VORTICES IN SEPARATED TURBULENT FLOWS

E. Schülein and V. Trofimov[1]
German Aerospace Center DLR, Institute of Aerodynamics and Flow Technology,
Bunsenstr. 10, 37073 Göttingen,
Germany

OVERVIEW

The study of the longitudinal vortex development in high-speed turbulent separated flows caused by relatively small irregularities at the model leading edges or at the model surfaces is presented in this paper. Experiments by means of oil-flow visualization and infrared thermography were conducted at Mach numbers 3 and 5 in the Ludwieg Tube Facility at DLR in Göttingen (RWG) with a model of a 2-D compression corner with deflection angles of 20°, 25° and 30°. The irregularities of the surface contour have been artificially simulated by very thin strips (vortex generators (VG) of different shapes and thicknesses) attached to the model surface. The dependence of the size and intensity of the observed longitudinal vortices on the introduced disturbances (thickness, shape and wavelength of the vortex generator strips) and on the flow parameters (Mach and Reynolds numbers, boundary layer thickness, compression corner angles etc.) has been shown experimentally. The transverse sizes of the generated vortices demonstrate certain “natural” scaling by local flow conditions.

1. INTRODUCTION

Streamwise vortices are frequently companions of different external and internal flows. The importance of studies of such vortices in boundary layers is based not only on the far-reaching effects in practical applications with distinct crossflow variations in surface heat, shear stress and pressure loads, but also on entirely fundamental interest in flows with complicated topological evolution. Such flows give a good example for long-term preservation and development of disturbances in fully turbulent flows. It is well known that steady longitudinal vortices can be evoked by any noticeable discontinuities at the leading edges or in the vicinity of obstacles on the surfaces [1]. The investigations [2-5] showed that not only “macro” irregularities in the leading edges, but also smallest “micro” discontinuities or notches could lead to such vortices in laminar flows. The existence of the counter-rotating streamwise vortices in regions with adverse pressure gradients in cases with and without flow separation was shown by surface flow visualizations, as well as by flow-field measurements.

The explanation for the nature of this phenomenon used most often is based on Görtler’s theoretical results [6, 7]. His physical model predicts the formation of longitudinal counter-rotating vortices in flows with concave streamline curvature evoked through centrifugal instability. The wall-curvature is really not necessary for this. For example, the observations of these vortices in laminar flow on a planar surface downstream of the incident-shock induced separation and reattachment [8-10] have shown that the streamline curvature, necessary to produce Görtler-like vortices, emerges by reattaching of the free shear layer. This concave curvature controls the intensity of vortices and consequently the levels of typical local heat flux peaks in the reattachment region and downstream of it.

The generation of similar quasi-steady longitudinal vortices in *turbulent* separated flows is a controversial fact. Despite large volume of different experimental studies, in which clear manifestations of streamwise structures in turbulent flows were obtained (see references in [11]), to date, many authors still hold to the view that long-living streamwise structures can not exist in turbulent flows (see e.g. [12],[13]). The reason is that the long-term preservation of longitudinal disturbances in turbulent flows seems to be in contradiction with the traditional point of view regarding turbulence as a high-viscosity system in contrast to laminar-flow systems. Recall that this concept is related to the generation of large-scale turbulent vortices immediately from the mean motion, followed by subsequent fragmentation of these vortices into smaller vortices. The transfer of energy here proceeds in a cascade (direct cascade) from large vortices to small vortices, with subsequent dissipation of the energy into heat. This process is expected to provide for dissipation of a disturbance initially generated by the vortex generator. Note that no such contradiction emerges in the case of laminar flow, since the viscosity in such a flow is three orders of magnitude lower than in turbulent flow, and the lifetime of large-scale disturbances here is therefore rather long. Yet, in turbulent flows situations are known, in which a reverse cascade of turbulent energy is observed. For instance, this type of energy transformation occurs in two-dimensional ocean turbulence where it gives rise to gigantic vortices [14]. The same process, which can be adequately predicted by the model of helical atmospheric turbulence, gives rise to hurricanes and typhoons ([15], [16]). In all these situations, turbulent vortices seem to transfer mechanical energy in the opposite direction, from small vortices to larger vortices (reverse cascade).

Another well known effect of isolated roughness elements or smallest discontinuities at the model’s leading edges is to cause early boundary layer transition (see e.g. [14]). The question about the possible cohesion of these two effects – tripping of laminar boundary layer and generation of longitudinal vortices downstream in turbulent boundary layers, was not clarified up to now.

[1] Novosibirsk State Pedagogical University (NSPU), Novosibirsk, Russia

The present work is a continuation of the experimental investigations [11], where the possibility of artificial generation of longitudinal vortices in fully turbulent separated flows by very weak disturbances was demonstrated in wind-tunnel tests. The experiments [11] were conducted in the Ludwieg Tube Facility at DLR Göttingen at Mach number M_∞ = 3 and Reynolds number $Re_x = 9\times10^6$ on a 20° compression corner model (FIG 1).

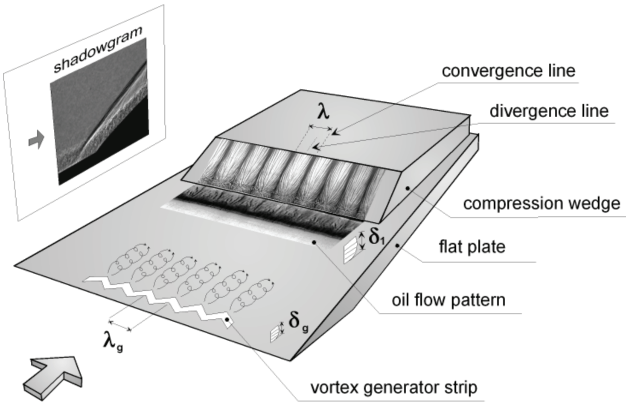

FIG 1. Sketch of the test model (flat plate / compression wedge - configuration with vortex generator strips at the leading edge), shadowgram and oil flow visualization pattern obtained in [11]

Investigations [11] have clearly demonstrated that by thorough preparation of the leading edges any chance for the initiation of stationary streamwise structures can be eliminated: the flow field in the region of re-attached flow over a compression wedge installed on a flat plate is quite two-dimensional (FIG 2a). Installation of periodic (equally spaced) low profile vortex generators (LPVG) near the leading edge of the flat plate leads to the formation of longitudinal vortex structures in the reattachment region at distances up to over 10^4 thicknesses of the VG (FIG 2b). The attachment of the zigzag strips from self adhesive 30..50µm-thin foil near the model's leading edge leads to the formation of longitudinal vortices in the reattachment region of the ramp, which was mounted in the fully developed turbulent boundary layer 380mm downstream (see FIG 1). The spanwise locations of the vortex pairs agree exactly with the locations of the rearmost points of the zigzag strip trailing edges ("teeth"-tips). The observed structures show for the model configuration and vortex generators investigated always a common divergence line for each vortex pair.

Extensive numerical investigations conducted later in [19] could confirm this behavior in most details. These numerical simulations were performed with the Navier-Stokes code CEVCATS-N for the same model geometry and similar flow conditions. With the help of both experimental and numerical examinations some properties of the flows concerning the possibility to generate longitudinal vortices in fully turbulent separated flows were developed in [20] and [21]. However, some discrepancies in these numerical and experimental results were found. Contrary to the experimental observations, the properties simulated numerically show e.g. a "*phase shift*" in the location of longitudinal vortices downstream of the VGs. So, typical for all cases investigated numerically is the formation of vortex pairs with a common convergence line downstream of each "teeth"-tip. As mentioned above, the vortex pairs observed experimentally in [11] show a common divergence line at this position.

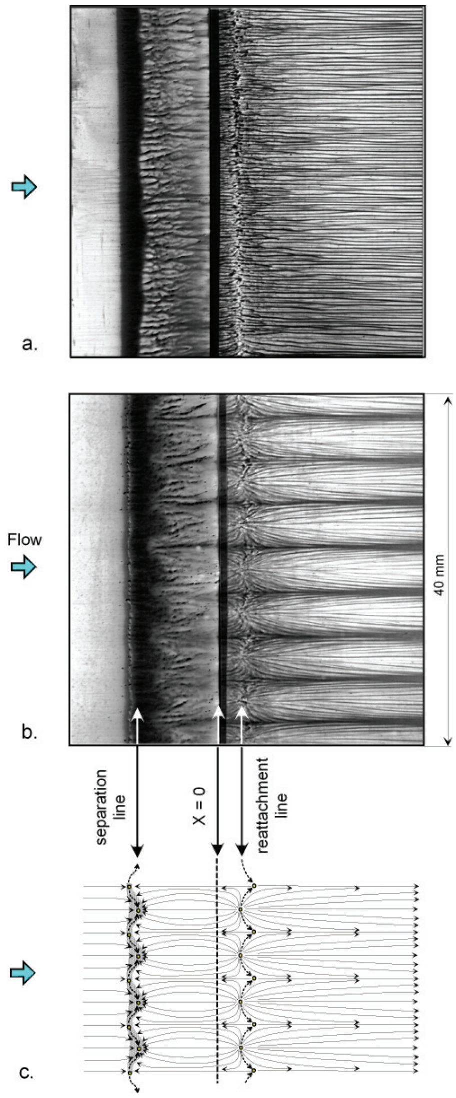

FIG 2. Flow pattern in the vicinity of the compression corner 20° at Mach 3 [11]: a) flow with artificially generated longitudinal vortices; b) sketch of the limiting streamlines; c) flow without vortex generators

The variation of the generator-to-generator or teeth-to-teeth spacing in the wind tunnel tests [11] clearly showed that the generated vortex pairs have always retained a certain common wavelength and are not free scalable at fixed flow conditions. For a wavelength of the disturbance that is essentially bigger as the characteristic wavelength of the vortex pair, the gap between neighboring ones was filled with 2D flow. This value of the VG spacing corresponds to the double diameter of the dominant longitudinal vortices and is approximately equal to the incoming boundary layer thickness immediately upstream of the separation zone. Contrary to the experimental observations, the numerical results [19] show only a weakening of the vortex effects for bigger generator-to-generator spacing, but not the formation of bounded vortices, which only fill a part of the distance between two vortex generators.

These disagreeing experimental and numerical results as well as the open questions about the influence of the introduced disturbances (thickness and shape of the VGs) and the flow parameters (Mach and Reynolds numbers, boundary layer thickness etc.) on the size and intensity of the observed longitudinal vortices stimulated this new experimental study. The aim of the work is to find final confirmations for ambiguous topics, as well as to examine the idea about the existence of a natural wavelength of the streamwise vortices, which grows with the boundary layer thickness depending on the other crucial parameters.

2. EXPERIMENTAL PROGRAM

2.1. Test model and flow conditions

The test model configuration for the present investigations is based on the flat plate with a sharp leading edge (thickness of about 0.1mm) and was 500mm in length and 400mm in width (FIG 3). The compression wedge plate (300mm in length and 400mm in width) with deflection angles of 20°, 25° and 30° could be mounted on the main plate at different locations so that the distance between its leading edges x_s lies between 225mm and 475mm. The thicknesses of the main plate and the compression wedge plate were 20mm.

The nominal free-stream conditions in the test section were at Mach number $M_\infty = 3$: stagnation temperature $T_0 = 260$K, stagnation pressure $P_0 = 0.32$MPa, unit Reynolds number of about $Re_{1\infty} = 30\times10^6$/m; and at $M_\infty = 5$ correspondingly: $T_0 = 410$K, $P_0 = 2.55$MPa, $Re_{1\infty} = 45\times10^6$/m. The former measurements of the boundary layer properties on the flat plate model without VG's ([23], [24]) showed a well-developed, 2-D turbulent boundary layer in the investigated region at given conditions.

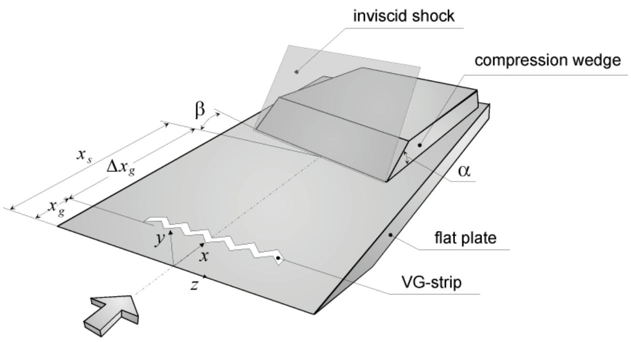

FIG 3. Sketch of the test model

3. EXPERIMENTAL RESULTS AND DISCUSSION

3.1. Flat plate reference flow with and without vortex generators

The aim of the first part of investigations was mainly the detection of surface footprints in the incoming boundary layer upstream of the separation zone as well as in the reattachment region, which stem from disturbances artificially generated by vortex generators. The measurements by IR-Thermography were conducted to compare the heat transfer distributions on the basic flat plate with and without vortex generator strips. The compression ramp was completely removed from the model.

FIG 4 shows the results of heat flux measurements on the flat plate with and without vortex generators at Mach 5. The heat flux distribution was obtained in two separate wind-tunnel runs and demonstrates a total area of about 95×140mm². The heat flux rates here are normalized by the reference value and the color scales used are identically, allowing a direct comparison of the results. The flow direction is from left to right.

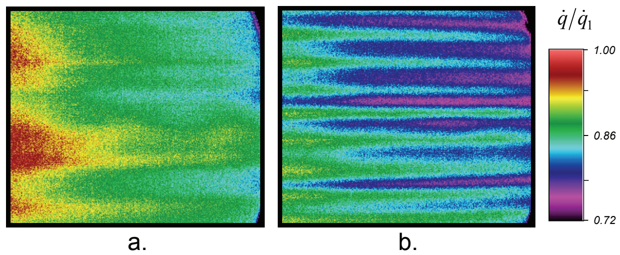

FIG 4. Heat flux distribution on the flat plate without a ramp at $M_\infty = 5$: a) without vortex generators; b) with strip-LPVG (x_g = 5 mm, h_g = 0.2mm, λ_g = 11.3mm). The location corresponds to variation of Re_x from 15.6×10^6 to 22.0×10^6

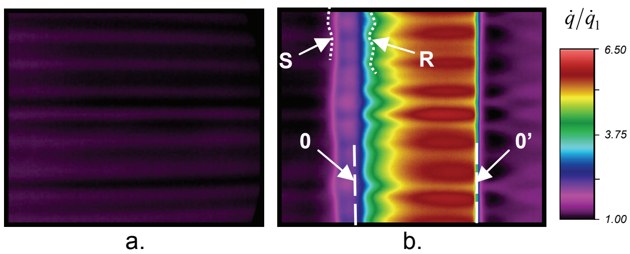

FIG 5. Heat flux distribution at $M_\infty = 5$ & x_g = 5 mm, h_g = 0.2mm, λ_g = 11.3mm: a) on the flat plate (the same as in FIG 4b); b) on compression corner 25° at $Re_x = 19.6\times10^6$

It can be seen that the heating rates without vortex generators (FIG 4a) decrease monotonously with distance from the leading edge as expected for turbulent boundary layer flows. Some global 3D-uneveness is originated by residual leading edge and free-stream irregularities. The results of heat transfer measurements at the same flat plate in the presence of zigzag generator strips near the leading edge show a fully different behavior (FIG 4b). Namely, a row of distinct streamwise structures are visible downstream of the zigzag LPVG-strips along the flat plate surface up to the biggest investigated distances from the leading edge. That is a very important finding, which is a convincing confirmation that the vortex generators used cause a generation of visible longitudinal vortex structures in the incoming boundary layer upstream of the separation zone. These vortices are obviously enhancing later on the reattachment region and become visible in the main flow parameters. The results complete and confirm the ideas of the former examinations [15] and [39]. An exemplification of this thesis can be found in FIG 5, which shows heat flux distributions resembling the flow on the flat plate with and without the compression wedge of α = 25°. The distribution in FIG 5b show some important flow features typical for separated flows. Those are the incoming flow with low heat flux levels, the separation zone between the meandered separation (S) and reattachment (R) lines, the flow region downstream of the reattachment region on the compression-wedge (0) with clear longitudinal structures, and, finally, the flow region downstream of the external corner (0'), where the traces of the streamwise structures are retained. The traces of streamwise structures, which are visible in the incoming boundary layer, can be observed as continuation in the separation and reattachment regions.

3.2. On the nature of long-living streamwise vortices in turbulent flows

The fundamental problem mentioned above is that longitudinal disturbances, weak in intensity but finite in scale, are retained far downstream under the conditions of turbulent flows to be sharply amplified in the regions with local pressure gradients. The question is: why fails the turbulent momentum-transfer in the boundary layer to dissipate low-intensity disturbances of the mean velocity field?

One of the key phenomena should be analyzed here is, to the authors' opinion, the tripping effect of roughness elements. As mentioned above, steady longitudinal vortices can be evoked by any noticeable discontinuities in the leading edges or in the vicinity of micro-obstacles on the surfaces. On the other hand, all these disturbances lead also to early transition due to laminar flow contamination. Very detailed recent review of roughness effect on laminar-turbulent transition can be found in [14]. As shown there on the results obtained e.g. in [28], the roughness affects the transition location if the roughness size becomes larger than the necessary 'critical' value (FIG 6, data 2).

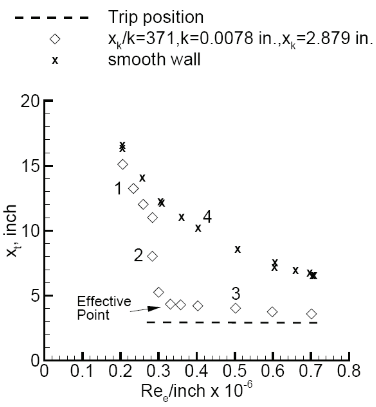

FIG 6. Variation of transition location with unit Reynolds number on a 5° half-angle sharp cone at M_∞ = 2.71 (results [28] cited from [14])

The roughness is termed *"effective"* when it tripped the boundary layer as effective as possible (FIG 6, data 3). At smaller roughness size the transition location tracked the smooth wall value (FIG 6, data 4) at a something lower level (data 1). The difference in the transition locations for *"ineffective"* small roughness and for a smooth wall is noticeable, because of even at these "*undersized*" roughness elements, each of them generate a wake with streamwise vorticity, which growth via known instability mechanisms and lead finally to the something earlier transition inside of a turbulent wedge [14].

The visualization of the transition process with single turbulent wedges stimulated by isolated roughness elements is presented in FIG 7 quoted from [14]. The contamination in the wake of triangular trips starts at different distances downstream of them (shown by arrows) dependent on the local thickness of the boundary layer at the trip location.

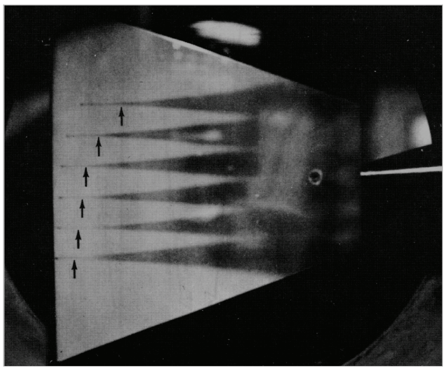

FIG 7. Effect of boundary layer tripping by triangular trips (VGs) visualized using Fluorene sublimation (results [27] cited from [14])

The idea proposed in the present work is to appreciate the influence of these steady turbulent wedges, which exist always in the wakes of the isolated vortex generators or roughness elements, on the additional amplification and invigoration of the longitudinal vortices generated upstream. This amplification effect is due to the development of semi-conical displacement bodies (turbulent wedges) inside of the incoming 2-D laminar flow with a consequently creation of favorable streamline curvature in the outer parts of the boundary layer. Such a "on the way refueling" may be one of the reasons that the longitudinal vortices investigated can hold out the relative big distances and become again visible in regions with concave streamline curvature in fully turbulent flows.

The other more abstract explanation of the long-term preservation of vortical disturbances in turbulent flows could be the *reverse cascade energy transfer* mentioned above. It can be speculated that the preservation of generator-induced disturbances happens due to the energy replacement from the turbulent motion that proceeds according to the reverse-cascade scheme. From the point of view propagated to explain e.g. the helical turbulence effects [22], such a situation is possible, because the scale of generator-induced disturbances is comparable with the largest turbulent vortices. Note that the permissibility of the reverse transfer of mechanical energy from small to large vortices is, at least at the moment, controversial.

3.3. Influence of the relative size of the single LPVGs on the downstream flow topology

The influence of the relative size of a single prism-VG on the flow topology generated downstream near the ramp has been investigated by varying the generator's height h_g and span (or width) a_g, as well as the distance x_g. The base shape of the prism VG used was an equilateral triangle. The results of limiting streamline visualizations for different combinations of geometry parameters are presented qualitatively in FIG 8.

The streamline patterns explain the different mechanisms of vortex generation with variation of the relative horizontal and vertical dimensions of the LPVGs. The dimensions of the prism are specified relatively to the boundary layer thickness. The expressions for “recompression” (A) or “horseshoe” (B) vortex pairs were used in the wake if the obstacle indicates the cause of its generation. The origin of these vortex pairs can be found in corresponding separation regions. The reason for the A-type vortex generation is the swept recompression shock-wave/boundary-layer interaction in the wake flow. More details to flow structure in the wake of a single high fin at supersonic speeds can be found e.g. in [25]. The well-known horseshoe separation near blunt obstacles is a cause for the generation of B-type vortex pairs. Thus, according to that the relative wide and high prisms generate three vortex pairs (FIG 8a): one “recompression” (A) and two “horseshoe” pairs (B).

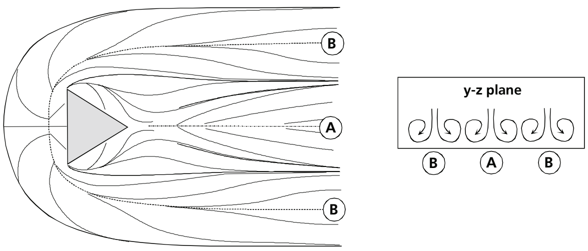

a. wide & high vortex generator

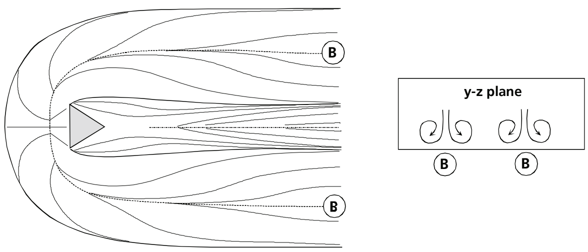

b. high low-span vortex generator

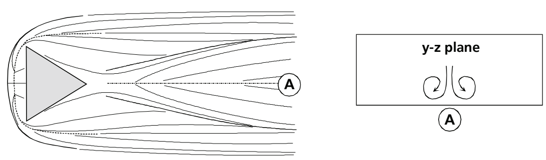

c. low-heigth vortex generator

FIG 8. Mechanism of vortex generation at supersonic speeds by a single prism VG (A – «recompression» vortex pair, B – «horseshoe» vortex pair)

Additionally to the most common combination of A and B vortex structures, presented in FIG 8a, at least two other special cases for smaller VGs can be defined. Hence, the relatively high but low-span obstacles generate two very intense B-type vortex pairs (FIG 8b), which suppressed the development of the A-type vortex pair in the recompression region because the spanwise distance is too small between those. For the low-height obstacles, where the horseshoe vortices are very weak from the beginning, the development of the recompression vortex pair happened free (FIG 8c).

The last two “special” cases have been observed in the experiments presented in FIG 9. For a low-height vortex generator (h_g = 0.05mm at x_g = 5mm, FIG 9a) the results demonstrate the footprint of a pair of streamwise vortices (A) with a longitudinal divergence line shedding from the rear corner of the triangular generator. The footprint of the vortex pair is embedded between two longitudinal convergence lines. The dominated vortex pair is illustrated in FIG 9 by a big arrow and the suppressed pair – by the smaller ones. This differentiation has only relative character and is not a scale of absolute vortex pair intensity. The increase of the generator’s height h_g up to 0.2mm (FIG 9b) yielded a new type of flow structure on the ramp with two pairs of streamwise vortices (B-B). The later displacement of this “higher” vortex generator (h_g = 0.2mm) to the location x_g = 75mm with “thicker” local boundary layer shows the coming back of the vortex structure to the primary as shown in FIG 9a. These experiments proved the existence of a critical value for the ratio h_g/δ_g for a single VG. Above this, the flow past the generator changes the type of topology.

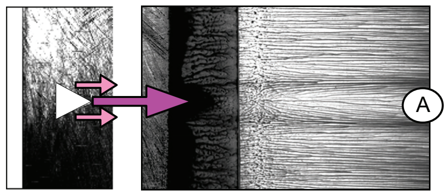

a. h_g = 0.05mm

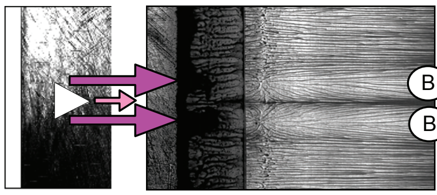

b. h_g = 0.2mm

FIG 9. Left-side: leading edge of the plate (single VG, x_g = 5mm, $a_g = b_g$ = 5mm); Right-side: oil-flow pattern on the 2-D compression corner

Consequently, the existence of a critical value for the h_g/δ_g ratio for single VG, and the cast into a different flow topology behind the generator, does not mean a clear jump but a sooner restructuring. The discussion about the lowest thickness of an effective vortex generator [14] show that the value $h_g^+ = u_\tau h_g / \nu$ could be a more general parameter than h_g/δ_g. The analysis of the present data shows that the switch between both different vortex structures happens at values of h_g^+ between 10 and 20.

As shown in [14], the most well accepted correlation parameter for the effects of roughness on transition is the roughness Reynolds number defined as $Re_k = U_k k/\nu_k$, where k is the roughness size, U_k *and* ν_k – are the velocity and viscosity of the flow at the edge of the roughness element. In the variables of the present work the Re_k can be rewritten by $Re_g = U_g h_g/\nu_g$. The most important difference between Re_g and h_g^+ mentioned above is obviously the using local velocity U_g instead of friction velocity u_τ. Which of these two parameters is more suitable as correlation parameter for prediction of vortex topology generated by the LPVG should be analyzed further.

3.4. "Natural" scale of longitudinal vortex pairs

The investigations of the generator's wavelength λ_g effect in [11] clearly showed that the generated vortex pairs have always retained a certain common wavelength λ and are not free scalable for fixed flow conditions. For λ_g that is essentially bigger as λ, the gap between neighboring ones was filled with 2D flow or with additional weaker vortices. If λ_g was essentially smaller as λ, then all vortex tracks practically vanish from oil flow pattern. The value of λ could be determined in [11] for given conditions approximately between 4.9 and 5.7 mm. This value of the VG spacing corresponds to the double diameter of the dominant longitudinal vortices and was approximately equal to the incoming boundary layer thickness δ_1 or somewhat bigger. The lower limit for the ratio λ_g/δ_1, below of which no vortex could be generated artificially, is given in [11] with approximately 0.8 – 0.9. Note, these investigations were made at constant ramp location on the plate and a corresponding constant boundary layer thickness δ_1. Consequently, the statement over the relative distance λ_g/δ_1 has no general validity and should be clarified by variation of the boundary layer thickness.

The numerical investigations [19] confirmed that for a series of investigated wavelengths (3mm, 6mm, 9mm and 12mm) the generated vortex pairs become most intense for a generator wavelength of 6mm. For smaller and bigger wavelengths the vortex effects at the reattachment areas of the ramps weakens and the "natural" scales of vortex pairs could not be derived from these results.

The experimental investigations of hypersonic reattaching flows [8] have shown the effect of the boundary layer thickness on the diameter of longitudinal vortices downstream of the incident shock / laminar boundary layer interaction. The longitudinal vortex diameters were approximately equal to the thickness of the undisturbed laminar boundary layer at the impingement position of the incident shock. The second important result of these investigations was the fact that the local heat peaks in the reattachment region increase with stronger impinging shock waves and with lower Reynolds numbers. An effect of the shock intensity on the longitudinal vortex diameter could not be found. It must be considered that the investigated vortices were not artificially generated in these tests but, as declared by the authors in [8], seem to be initiated by very small leading edge inaccuracies. In some tests, the vortex spanwise locations were reproducible and fixed on the model. Hence, the results of vortex diameter examinations could clearly be influenced by it.

A list of factors, which can have an influence on the spanwise dimensions of longitudinal vortices in the reattachment region of a compression wedge located at distance Δx_g from the trailing edge of the VG, can be compiled based on obtained and available data of streamwise structures. The natural scale or wavelength of longitudinal vortex pair λ depends, in general, on the local boundary-layer thickness and on a set of external factors:

$$\frac{\lambda}{\delta_1} = f\left(M_\infty, \mathrm{Re}_\infty, \frac{\Delta x_g}{\delta_g}, \frac{x_g}{\delta_1} (or\ \frac{x_s}{\delta_1}), \frac{h_g}{\delta_g}, \frac{\lambda_g}{\delta_1}, \frac{p_2}{p_1}, \alpha, \beta, \frac{T_g}{T_0}, VGT \right).$$

Here, λ_g is the generator-to-generator spacing, h_g is the height of the vortex generator, δ_g and δ_l are the boundary-layer thicknesses at the generator's and ramp's location for the undisturbed flat plate boundary layer, p_2/p_1 is the shock strength, α and β are the deflection and yawing angles of the ramp, T_g/T_0 is the ratio of the generator's temperature and total temperature, VGT is the used vortex generator's type or configuration, x_g – distance between the VG's and the plate's leading edges, and $x_s = \Delta x_g + x_g$.

3.4.1. Effect of the boundary layer thickness at the shock position

The dependence of the wavelength on the boundary layer thickness was already presumed since the discovery of the longitudinal structures. But the known approximations were not systematic and did not take into account all influencing factors. That is the reason why in the present investigations no comparisons with other data were carried out.

The new results obtained in the present work confirm the described statements and show that the local thickness of the boundary layer is one of the most important scaling parameters. In fact, depending on the spatial frequency of the generators three topologically different flow patterns in the shock wave / boundary layer interaction region can be observed: a two-dimensional flow without generated vortices, flow with narrowly packed up streamwise structures, or a pattern that reveals the natural scale of streamwise structure on the background of a quasi-two-dimensional flow. The last flow pattern allows the evaluation of the natural scales of the longitudinal vortices.

FIG 10 (right photos) shows distinct footprints of longitudinal structures on the 25° compression wedge installed at different distances x_s. The left photo shows always the used zigzag generator strip with λ_g = 11.3mm and h_g = 0.05mm. The vertical silver line in this photo near the leading edge of the generator strip marks the distance x_g = 5mm. All these visualizations display the existence of natural scales for the cross-diameters of the generated streamwise vortices. For each pattern, two groups of topologically similar sub regions in the structure of the limiting streamlines are observed. In the first one, the streamlines describe footprints of a vortex pair. In the other, streamlines are almost quasi-parallel to each other and display almost a 2D-flow situated between vortex pairs. It can definitely be seen that the wavelength of the vortex-pairs climbs with the distance x_s and correspondingly with the local thickness of the boundary layer upstream of the compression wedge.

This effect was confirmed also by the results of heat flux measurements for different wedge locations downstream of the low-profile VG. FIG 11 shows the normalized distributions of heat flux rates at two different x_s = 225 and 325mm. These tests with periodic generators of h_g = 0.05mm and λ_g = 11.3mm and the compression wedge of 20° revealed distinct longitudinal structures. The natural size of the vortices and the gaps between them (FIG 11a) are seen to be in a good agreement with oil flow visualization data. At bigger distance between the vortex generator and the compression wedge (FIG 11b) the cross sectional size of each vortex-pair's footprint becomes larger.

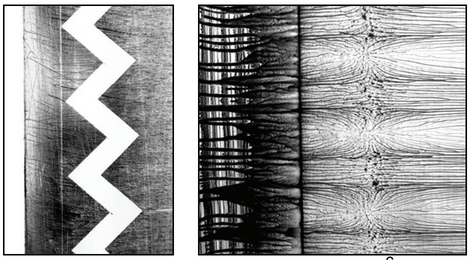

a. x_s = 225 mm (Re_x = 5.85×10^6)

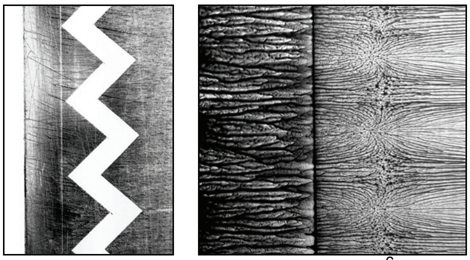

b. x_s = 275 mm (Re_x = 7.15×10^6)

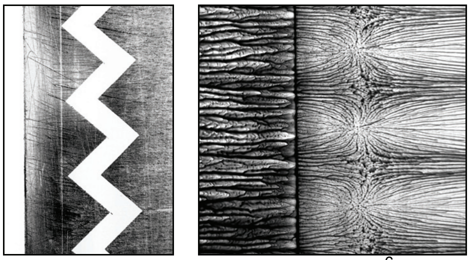

c. x_s = 325 mm (Re_x = 8.45×10^6)

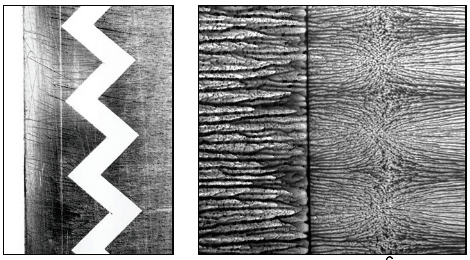

d. x_s = 375 mm (Re_x = 9.75×10^6)

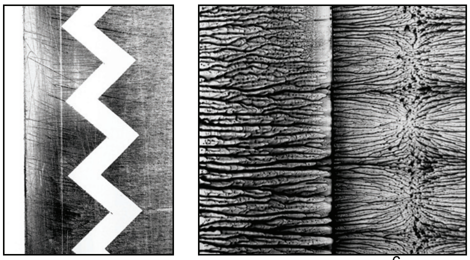

e. x_s = 475 mm (Re_x = 12.35×10^6)

FIG 10. Left side: strip VG, λ_g = 11.3mm, h_g = 0.05mm, x_g = 5mm; Right side: 2D-compression corner at α = 25°, M_∞ = 3 and different distances x_s

3.4.2. Effect of the compression corner angle

The development of Görtler-like vortices in laminar flows at different ramp deflection angles has been considered previously in [2-5,12,13] just from the standpoint of promoting the laminar-turbulent transition. With the increase of α between 10 and 20 degrees, the longitudinal vortices in the laminar flow gradually decay as turbulence develops in the flow. The effect on the vortex diameter could not be extracted in these works since the vortices were not artificially generated and the obtained wavelengths were influenced by the real leading edge contour.

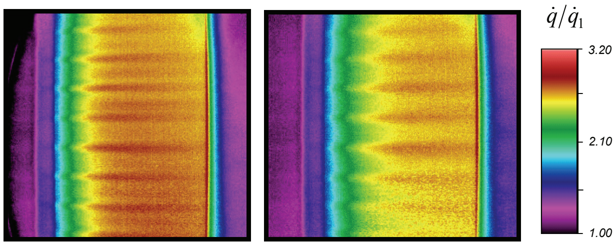

a. b.

FIG 11. Heat flux distribution on the compression corner of 20° at M_∞ = 3: a) Re_x = 5.85×10^6 (x_s = 225 mm); b) Re_x = 8.45×10^6 (x_s = 325 mm)

The effect of the compression angle on the intensity and transverse size of streamwise structures is illustrated in FIG 12 for the compression angles of 25° and 30°, respectively. The properties of surface heat-flux distributions agree fairly well with oil-flow visualization data. Most distinctly to be seen is the extension of the separation region near the compression wedge and the increase in the intensity and scale of the streamwise structures with increasing compression angle.

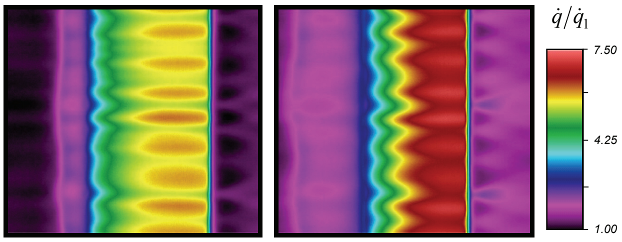

a. α = 25° b. α = 30°

FIG 12. Heat flux distribution on compression corner at M_∞ = 5 & Re_x = 19.5×10^6 at different α

The dependencies of the obtained "natural" wavelengths (or cross sectional size of vortex pairs) λ on the distance x_s and on the local boundary layer thickness δ_1 for α = 20° and 25° are shown in FIG 13 and FIG 14. The attempt to obtain quantitative data for α = 30° failed unfortunately. These data are more difficult to interpret because the separation region near the 30°-compression wedge is extremely enlarged and partially show large-scale three-dimensional effects. The values for δ_1 at investigated x_s-distances were calculated by simplified empirical correlations, which are proposed in [26] for turbulent flows. The agreement of the values that were obtained with single triangle-prism VGs and with "zigzag" strip VGs at α = 25° is very remarkable.

The effect of the compression angle α on the wavelength λ turned out to be most pronounced as is shown in the graph in FIG 13. The obvious increase of the wavelength λ with the change of the compression angle α from 20° to 25° is significant. The very strong dependence shows that not only the boundary layer thickness is responsible for the wavelength scaling. Moreover, the increase of the vortex wavelength with the thickness of the boundary layer for a wedge angle of 25° is approximately twice as high as in the case of α = 20°. Consequently, the relation of the wavelength to the boundary layer thickness λ/δ_1 shows the dependence on the compression angle α (FIG 14).

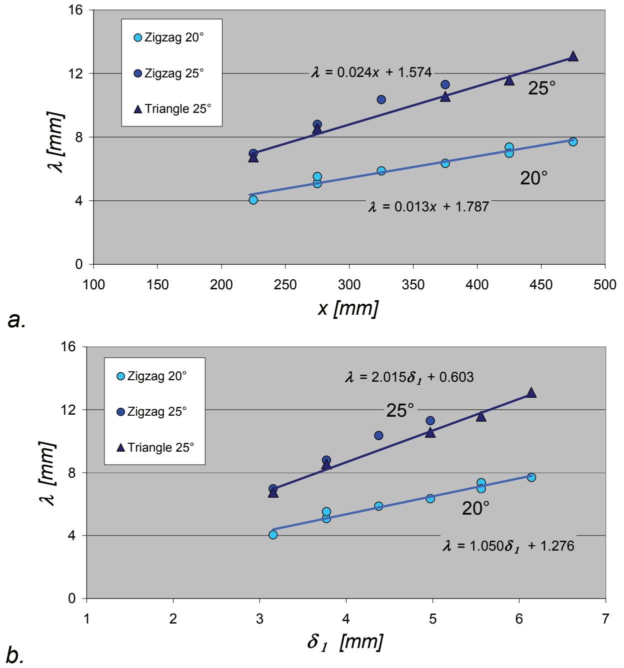

FIG 13. Effect of compression angle and boundary layer thickness at Mach 3: a) λ vs. x_s; b) λ vs. δ_1

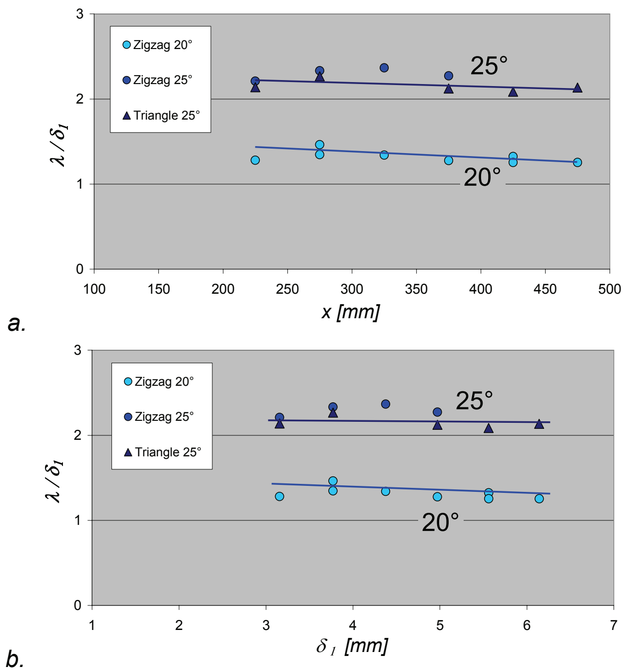

FIG 14. Effect of compression angle and boundary layer thickness at Mach 3: a) λ/δ_1 vs. x_s; b) λ/δ_1 vs. δ_1

How does the compression angle influence the transverse size of streamwise structures? As shown above the initial disturbances from the LPVG, which is located near the leading edge, remain weak up to the compression-wedge location and subsequently amplify in the reattachment zone with formation of intense longitudinal vertical structures. With increase of the compression angle, the size of the separation zone increases as well as the streamwise pressure gradient and the absolute value of the pressure jump. Both factors amplify the generator-induced disturbance, and an increase in the vortex intensity and in the streamwise scale of the structures can be observed.

3.4.3. Effect of Mach number

According to [2 - 5], where the observations were gained from the ablation technique, the λ/δ_1 ratio was constant in a very wide range of Mach numbers M_∞= 1.5 – 7.0 and is noted approximately equal to 2.5. In other studies, mainly data for constant Mach numbers only were reported.

Most investigations of separation control reviewed in [29] were carried out at sub- and transonic speeds and therefore results about the influence of the Mach number exist only up to a Mach number of 1.6. The statement of the natural scale of the generated vortices can be derived from the information about the distance between two VGs, which was optimal for separation control purpose. The results show a strong dependency on the used VG's-typ as well as on the very short distances x_g but not on the flow speed. Hence, according to the analysis of existing data in [29], the values of λ/δ_1 for a most effective separation control in the whole Mach number range from 0.1 to 1.6, lie between 0.8 and 3.6 in all known investigations. These values are given here only as reference because the decision of the most effective distance λ_g was implied in cited investigations for most effective suppression of flow separation.

As mentioned above, the variation of the wavelength λ_g in [11] at Mach number M_∞ = 3 on a 20° compression corner model showed that the maximum spanwise intensity of generated vortices in the reattachment region could be determined for ratios λ/δ_1 of about 1 or more.

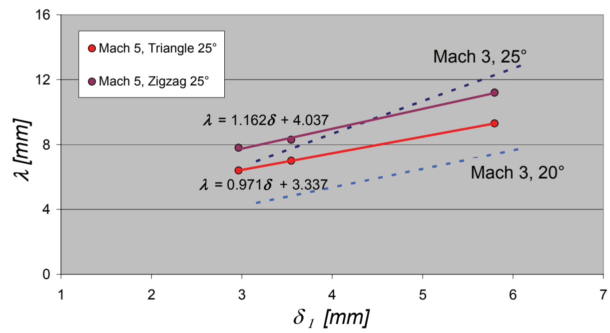

FIG 15. Mach number, local boundary layer thickness and compression angle effects on the wavelength of generated longitudinal vortices

The present investigations provide particular information on the Mach number effect. Thus, in FIG 15 the results obtained show the effect of Mach number and local boundary layer thickness on the wavelength λ_g for a compression angle α of 25°. For M_∞ = 3, an increase in the compression angle results in an increased transverse scale of streamwise structures. The λ-level along the x-coordinate shifts upwards; simultaneously, the slope of the curve increases. At M_∞ = 5, the slope for the compression angle α = 25° is approximately the same as for α = 20° at M_∞= 3, although the curve itself is shifted upwards. The data for both Mach numbers show an increasing scale of streamwise structures with increasing compression angle or shock intensity. The pure Mach number effect can not be extracted from other dependent effects like shock wave intensity or the size of the separation bubble.

4. CONCLUSIONS

The longitudinal vortical disturbances, which are initiated by leading edge or surface irregularities that represent a "hydraulic roughness", demonstrate a conservative behaviour up to very large distances within the fully developed turbulent flow. The investigations have shown that such streamwise vortices exist in turbulent supersonic flows on flat plates without pressure gradients over distances of the order of 10^4 vortex-generator heights. The interaction of the boundary layer with strong adverse pressure gradients accompanied by flow separation leads to the reinforcement of these disturbances and to further development of intense longitudinal vortex pairs in the reattachment region.

The total number, dimension, and type of installed vortex generators define the number of vortex pairs generated downstream. With the exception of a narrow region along the vortex outer limits, where weak "satellite" longitudinal structures can originate on the basis of viscous effects, a vortex pair cannot self initiate additionally neighboring vortex pairs if a corresponding vortex generator is missing in the upstream region. With other words, the disturbances caused are never transferred in the spanwise direction and develop only downstream in the wake within a certain corridor. The natural transverse size of this corridor and its sensibility to selected flow parameters are the object of the present investigations.

The most important results of the study can be summarized as follows:

1) The relative size and the type of the vortex generator determine the topology of the longitudinal vortex structures downstream in their wake region. It was found that the relative size of the VG have a critical influence on the resulting flow topology. The experiments show the existence of a critical value for the ratio h_g / δ_g of a single VG. With exceeding this ratio, the flow past the generator changes the type of topology. Hence, the vortical structure in the wake of a single triangular prism is different for "high and wide", "high low-span" and "low-height" vortex generators.
2) Two types of vortex pairs in supersonic flows were found: the "recompression" (A-type) and the "horseshoe" (B-type) vortex pairs. The A-type vortices emerge due to the recompression in the wake flow of vortex generator. The well-known horseshoe separation near blunt obstacles is a cause for the generation of B-type vortex pairs.
3) The transverse sizes of generated vortices demonstrate certain "natural" scales typical for local flow conditions. The local thickness of the boundary or shear layer is one of the most important scaling parameters for the characterization of natural scales for the generated vortex-pairs.
4) The intensity of the longitudinal vortices and the relative "natural" wavelengths λ / δ_1 decreases slowly with distance from the vortex generator and the model's leading edge x_s.
5) The vortex intensity and the streamwise "natural" scales of the structures are increasing with increase of the compression angle. The pure Mach number effect was analyzed but could not be extracted from other dependent effects like shock wave intensity or the size of the separation bubble.
6) The present study yields clear recommendations that enable the guaranteed elimination of longitudinal vortices by means of periodic generators with certain parameters. In order to avoid long-living longitudinal vortices on surfaces of wind tunnel models, periodic vortex generators should be chosen with wavelengths that are noticeably smaller than the boundary layer thickness in the investigated flow.
7) Two different mechanisms are analyzed to be responsible for the long-term preservation of steady longitudinal vortical disturbances in turbulent flows: the particular role of *steady turbulent wedges*, which exist permanently in the wakes of the isolated vortex generators or roughness elements, as well as the more speculative effect of *reverse cascade energy transfer* in turbulent boundary layers.

5. REFERENCES

[1] Pearcey H.H., "Shock Induced Separation and its Prevention by Design and Boundary Layer Control", Boundary Layer and Flow Control, Vol. 2, edited by Lachmann G.V., Pergamon, New York, 1961, pp.1277-1312.
[2] Ginoux, J.J., "Experimental evidence of three-dimensional perturbations in the reattachment of a two-dimensional laminar boundary layer at M = 2.05", TCEA TN1, Training Center for Experimental Aerodynamics, Rhode-Saint-Genèse, Belgium, November 1958.
[3] Ginoux, J.J., "Laminar Separation in Supersonic Flow with Emphasis on Three-Dimensional Perturbations at Reattachment," TCEA TN3, Training Center for Experimental Aerodynamics, Rhode-Saint-Genèse, Belgium, February 1960.
[4] Ginoux, J.J., "On Some Properties of Reattaching Laminar and Transitional High Speed Flows," VKI TN 53, VKI, Rhode-Saint-Genèse, Belgium, September 1969
[5] Ginoux, J.J., "Streamwise Vortices in Reattaching High-Speed Flows: A Suggested Approach," AIAA Journal, Vol.9, No.4, 1971, pp.759-760.
[6] Görtler, H. „Über eine dreidimensionale Instabilität laminarer Grenzschichten an konkaven Wänden", Nachrichten der Gesellschaft der Wissenschaften zu Göttingen, Mathematisch-Physikalische Klasse, Fachgruppe 1, Bd.2 (1940), pp.1-26. (in German)
[7] Görtler, H. „Instabilität laminarer Grenzschichten an konkaven Wänden gegenüber gewissen dreidimensionalen Störungen," ZAMM, Bd.21, Nr.4 (Aug.1941), pp.250-252 (in German)
[8] Henckels A., Kreins A.F., and Maurer F., „Experimental Investigations of Hypersonic Shock-Boundary Layer Interaction", Z. Flugwiss. Weltraumforsch., Vol.17, 1993, pp.116-124, Springer-Verlag, 1993.

[9] Kreins A.F., Henckels A., and Maurer F., „Experimental Studies of Hypersonic Shock Induced Boundary Layer Separation", Z. Flugwiss. Weltraumforsch., Vol.20, 1996, pp.80-88, Springer-Verlag, 1996.
[10] Domröse U., Krause E., and Meinke M., „Numerical Simulation of Laminar Hypersonic Shock-Boundary Layer Interaction", Z. Flugwiss. Weltraumforsch., Vol.20, 1996, pp.89-94, Springer-Verlag, 1996.
[11] Schülein E. „Experimentelle Untersuchungen zur Längswirbelbildung in turbulenten Überschallströmungen mit Ablösungen," DLR IB 224 – 02 A 12, DLR Göttingen, 2002, 32p. (in German).
[12] Vermeulen, J.P., Simeonides, G. "Parametric studies of shock wave boundary layer interactions in two-dimensional compression corners at Mach 6", VKI TN 181, VKI, September 1992.
[13] Simeonides, G. "Hypersonic Shock Wave Boundary Layer Interactions over Simplified Deflected Control Surface Configurations," AGARD-R-792, Special Course on Shock-Wave/Boundary-Layer Interactions in Supersonic and Hypersonic Flows, August 1993, pp.7-1 – 7-47, 1993.
[14] Kraichnan R.H. "Helical turbulence and absolute equilibrium," J. Fluid Mech., 1973, V.59, pp. 745-752.
[15] Moiseev, S.S., Sagdeev R.Z., Tur A.V., Yanovsky V.V., "Theory of Formation of Large-Scale Structures in Hydro-dynamical Turbulence," J. Exp. Theor. Phys., 1983, V.85, No.6(12), pp.1979-1987 (in Russian).
[16] Berezin Y.A., Hutter K., Zhukov V.P. Large-Scale Vortical Structure Supported by Small-Scale Turbulent Motions. Helicity as a Cause for Inverse Energy Cascade, Continuum Mech. Thermodyn., 1991, v.3, 127-146.
[17] Schneider S.P., "Effects of Roughness on Hypersonic Boundary-Layer Transition", AIAA-2007-305, 45th AIAA Aerospace Sciences Meeting and Exhibit, Reno, Nevada, Jan. 8-11, 2007.
[18] Schülein E. and Trofimov V. (2006): Longitudinal Vortices in Separated Turbulent Flows, DLR-Report IB 224 – 2005 A 17, DLR Göttingen
[19] Lüdeke H. "Untersuchungen von Längswirbeln in abgelösten hypersonischen Strömungen", DLR FB 2003-04, Braunschweig, 2003.
[20] Lüdeke H., Schülein E. „Simulation of Streamwise Vortices on Turbulent Hypersonic Ramps", Proceedings of the Second International Conference on CFD, University of Sydney, Australia, 15.-19.06.2002, 2002.
[21] Lüdeke H., Radespiel R., Schülein E. „Simulation of Streamwise Vortices at the Flaps of Re-entry Vehicles", AIAA 2004-0915, 42nd AIAA Aerospace Sciences Meeting and Exhibit, 2004.
[22] Berezin Y.A., Trofimov V.M. "Large-Scale Vortex Generation Driven by Non-Equilibrium Turbulence," Fluid Dynamics, 1996, v.31, no.1, 39-46.
[23] Schülein E., "Skin Friction and Heat Flux Measurements in Shock Boundary Layer Interaction Flows", AIAA-Journal, Vol.44, No.8, Aug. 2006, pp.1732-1741.
[24] Schülein E. „Qualität der Strömung nach der Nachbearbeitung der Überschalldüse „M = 3" des Rohrwindkanals des DLR in Göttingen," DLR IB 223 - 99 A 12, Göttingen, 1999, 23 p
[25] Schülein E., "Development and Application of the Thin Oil Film Technique for Skin Friction Measurements in the Short-Duration Hypersonic Wind Tunnel", New Results in Numerical and Experimental Fluid Mechanics IV, edited by C. Breitsamter, B. Laschka, and H.-J. Heinemann, Vol. 87, Notes on Numerical Fluid Mechanics and Multidisciplinary Design, Springer-Verlag, Berlin, 2004, pp. 407 – 414.
[26] Chappel P.D., „Some Correlations for the Turbulent Boundary Layer on a Flat Plate," The Aeronautical Journal of the Royal Aeronautical Society, Vol.74, May 1970, pp.393-396.
[27] Hicks R.M. and Harper W.R. Jr., "A Comparison of Spherical and Triangular Boundary-Layer Trips on a Flat Plate at Supersonic Speeds", Technical Memorandum TM-X-2146, NASA, December 1970.
[28] Van Driest E.R. and Blumer C.B., "Boundary-layer transition at supersonic speeds − three-dimensional roughness effects (spheres)", J. of the Aerospace Sciences, 29, pp.909-916, August 1962.
[29] Lin J.C., "Review of Research on Low-Profile Vortex Generators to Control Boundary-Layer Separation", Progress in Aerospace Sciences, 38, 2002, pp.389-420.